Ultraviolet radiation and clouds: Couplings to tropospheric air quality

Shelby Winiecki and John E. Frederick

Department of the Geophysical Sciences, University of Chicago, Chicago, Illinois, USA

Received 10 May 2005; revised 25 August 2005; accepted 22 September 2005; published 16 November 2005.

[1] Measurements of solar ultraviolet irradiance obtained by a Brewer spectrophotometer located in Chicago, Illinois, reveal a wavelength-dependent excess attenuation associated with cloudy skies beyond that expected from the column ozone amount. When each observation is expressed as a fraction of the irradiance that would have existed under clear skies, a quantity called the transmission ratio, values for a wavelength band near 305 nm are generally smaller than those for a band near 345 nm under dense cloud cover. Transmission ratios computed for wavelength bands near 310 nm and 315 nm lie in between those for the above wavelengths. The observations are consistent with absorption of radiation in the interstitial air of a cloud, while the magnitude and wavelength dependence are like those expected from ozone. A radiative transfer calculation shows that ozone amounts typical of the troposphere are accompanied by enhanced absorption when placed in a medium that is optically thick in scattering. This mechanism constitutes a coupling between tropospheric air quality and the attenuation of sunlight provided by cloudy skies in the chemically active ultraviolet portion of the spectrum.

Citation: Winiecki, S., and J. E. Frederick (2005), Ultraviolet radiation and clouds: Couplings to tropospheric air quality, *J. Geophys. Res.*, *110*, D22202, doi:10.1029/2005JD006199.

1. Introduction

[2] Ultraviolet sunlight drives the chemistry of the clean and polluted troposphere. As such, it is important to understand the magnitude and variability of solar spectral irradiance reaching the ground as well as the mechanisms that control the transmission of the atmosphere. Historically, much attention focused on the role of stratospheric ozone, although absorption and scattering in the troposphere are important as well. In a monthly averaged sense, backscattering of sunlight by clouds and haze can cause a significant reduction in ground-level irradiance, an effect whose magnitude varies with geographic location [*Frederick et al.*, 1993; *Bordewijk et al.*, 1995; *Schafer et al.*, 1996; *Seckmeyer et al.*, 1996; *Erlick et al.*, 1998; *Repapis et al.*, 1998; *Barnard et al.*, 2003]. In urban areas and regions downwind from them, enhanced levels of particulate matter and gaseous absorbers provide additional attenuation [*Bruel and Crutzen*, 1989; *Erlick and Frederick*, 1998].

[3] The work reported here examines a data set of ultraviolet solar spectral irradiance acquired by a Brewer spectrophotometer located in Chicago, Illinois. The objective is to assess the role of local cloudiness in controlling ground-level irradiance at wavelengths less than 350 nm, including the region of strong absorption by ozone at wavelengths shorter than 315 nm. The possibility that the attenuation associated with cloudy skies varies with wavelength is of particular interest.

0148-0227/05/2005JD006199$09.00

2. Instrumentation and Data Sets

[4] A Brewer spectrophotometer, located at the University of Chicago, latitude 41.79°N and longitude 87.60°W, was one of approximately 20 such instruments that composed the U. S. EPA's network managed by the National Ultraviolet Monitoring Center (NUVMC) at the University of Georgia. *Kerr et al.* [1985] and *Kerr and McElroy* [1995] have described the sensor, so that no detailed discussion is required here. Designed for routine operation, the instrument scans the wavelength region from 286 nm to 363 nm, where the quantity sensed is the downward solar irradiance on a horizontal surface including the direct and diffuse components, at a spectral resolution of approximately 0.6 nm. The instrument acquires data at 5° intervals of solar zenith angle (SZA) through much of the morning and evening, with more frequent scans near solar noon. Personnel from NUVMC performed calibrations of wavelength and instrument response, traceable to NIST standards, on a yearly basis. Automated tests with an internal mercury lamp checked wavelength calibration each day, and biweekly tests using external 50-watt quartz halogen lamps documented small changes in instrument sensitivity at times between the annual calibrations.

[5] The research reported here considers data collected from May through September of 2001, an interval that spans the period of the year when photochemical processes are most likely to create degraded urban air quality. We excluded 15 days from this set owing to instrument-related problems and potentially poor data quality. In addition, the analysis omits data collected at SZAs in excess of 62°. This was done as a precaution to avoid any angular response errors in the sensor at high solar elevations and to ensure comparability with irradiances computed by a radiative transfer model that

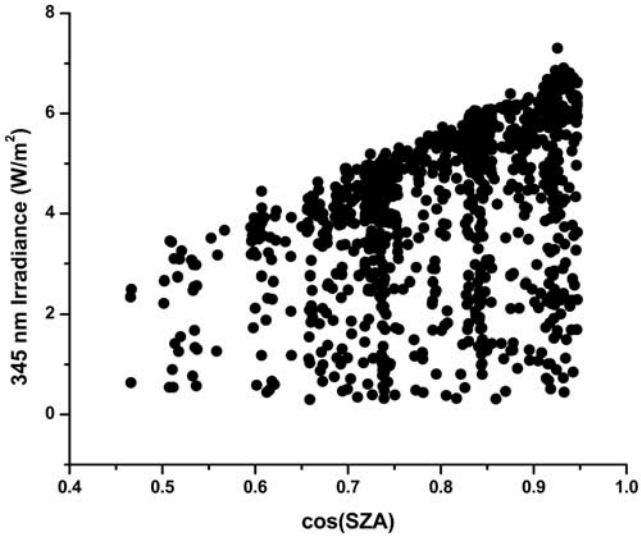

Figure 1. Solar irradiance measurements in the 345 nm band (340–350 nm) for the period May through September 2001 plotted as functions of the cosine of the solar zenith angle (SZA).

accounts for a spherical atmosphere in an approximate manner. After the above editing, the final data set consisted of 958 spectral scans over 138 days covering solar times from 9:00 hours to 15:00 hours.

[6] We selected measurements in four wavelength ranges for detailed analysis. These are the "305 nm band," defined as irradiance integrated over the range 303–308 nm, the "310 nm band" extending from 308–313 nm, the "315 nm band" from 313–318 nm, and the "345 nm band," encompassing 340–350 nm. We denote these measured irradiances by $E_M(\lambda, \theta)$ in watts m^{-2} where $\lambda = 305$, 310, 315 and 345 nm and θ is the SZA. Absorption by ozone is a major influence on ground-level irradiance in the shortest-wavelength band and decreases to become negligible in the longest spectra interval. Figures 1 and 2 present the irradiances measured in the 345 nm band and the 305 nm bands, respectively, expressed as functions of the cosine of the SZA at the time of measurement. The upper envelope of each plot corresponds to approximately clear skies, while the scatter at a fixed SZA is primarily a response to cloudiness. Variations in column ozone are an added contribution to variability in the 305 nm band.

3. Deductions Based on Measurements

[7] This section examines the measured irradiances to determine if they support the claim that cloudy skies provide an attenuation that depends on wavelength. The approach is statistically based because this allows us to identify specific relationships in the data even when other forms of variation are present. Furthermore, the conclusions are free of the need to use mechanistic radiative transfer models, which may introduce biases of their own into the analysis.

[8] As an initial hypothesis, assume that the attenuation of irradiance associated with a cloudy sky is independent of wavelength. This means that the effect of the cloud is to reduce the irradiance in each wavelength band to the same fraction of the clear-sky value. In this scenario, the irradiance ratios $E_M(\lambda, \theta)/E_M(345, \theta)$, where λ = 305, 310 and 315 nm, are independent of the presence of the cloud, although they still depend on the ozone content of the atmosphere. It is reasonable to assume an exponential relationship between $E_M(\lambda, \theta)/E_M(345, \theta)$ and the column ozone amount measured along the slant path of the direct solar beam. In this case, a plot of $\ln[E_M(\lambda, \theta)/E_M(345, \theta)]$ versus the corresponding slant path column ozone amounts will produce, to a good approximation, a straight line. Although the linear dependence is exact only for the direct component of sunlight, it still captures the general character of the relationship.

[9] Figure 3 depicts $\ln[E_M(305, \theta)/E_M(345, \theta)]$ as a function of slant path column ozone where the ozone

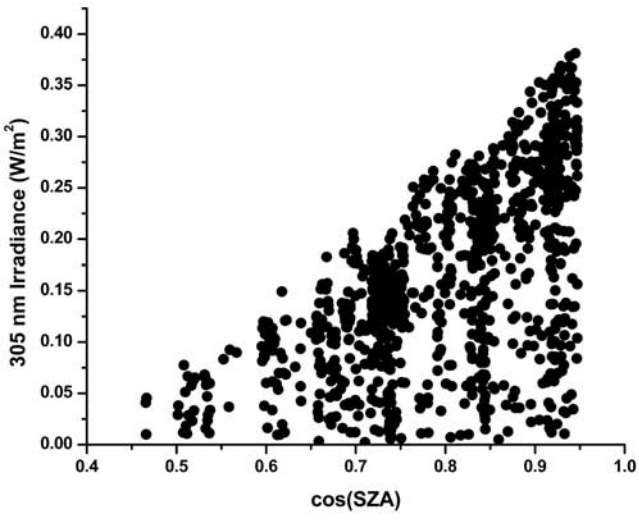

Figure 2. Solar irradiance measurements in the 305 nm band (303–308 nm) for the period May through September 2001 plotted as functions of the cosine of the solar zenith angle (SZA).

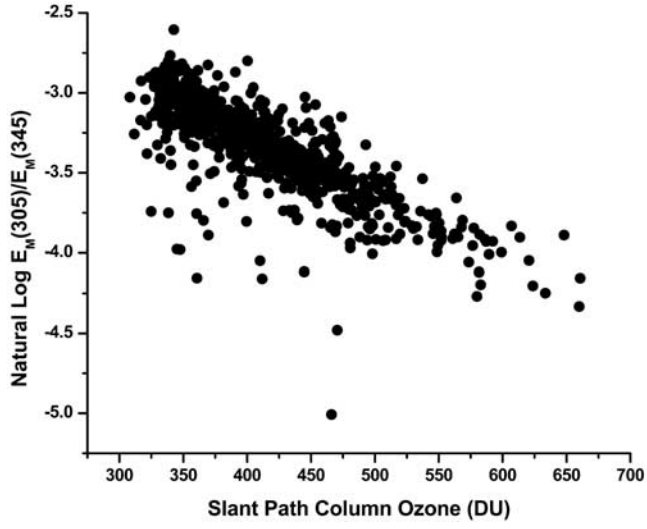

Figure 3. Relationship between the natural logarithm of the irradiance ratio $E_M(305, \theta)/E_M(345, \theta)$ and slant path column ozone in Dobson Units (DU). Results are based on measurements from the spectrophotometer.

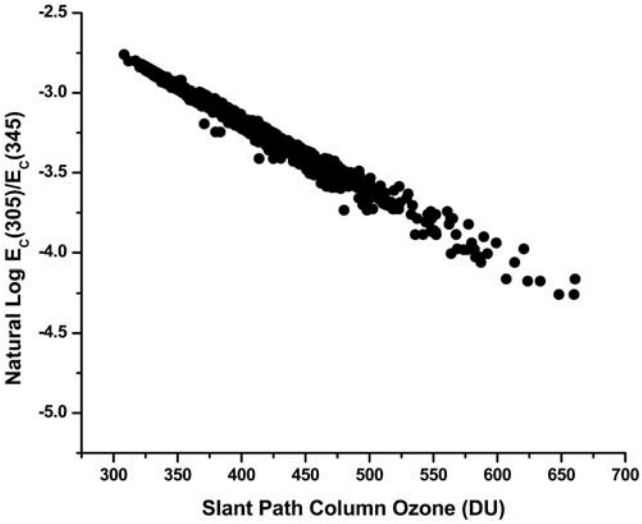

Figure 4. Relationship between the natural logarithm of the irradiance ratio $E_C(305, \theta)/E_C(345, \theta)$ and slant path column ozone in Dobson Units (DU). Results are based on radiative transfer calculations for clear skies using measured column ozone values are inputs.

amounts, in Dobson Units (DU), are from the Total Ozone Mapping Spectrometer (TOMS) on the Earth Probe satellite. The data are available from http://jwocky.gsfc.nasa.gov. A linear fit to the points in Figure 3 explains 68–69% of the variance in the dependent variable. For comparison, Figure 4 is the corresponding plot based on clear-sky irradiance calculations using the TOMS ozone values as inputs to the radiative transfer model described by *Frederick and Erlick* [1995]. In this case, a linear fit explains 98% of the variance. From Figure 4 it is evident that most of the scatter in Figure 3 does not arise from a deficiency in the linear assumption.

[10] The scatter in Figure 3 may arise from several factors, although an instrument-related cause is much less likely than geophysical sources. The noise level in the irradiance measurements, as determined from data obtained viewing artificial lamps, is less than 1% at the signal levels used here. This translates into negligible scatter on the vertical scale of Figure 3. As for geophysical causes, the column ozone amount on the horizontal axis may not be identical to what resided over the ground-based sensor at the time of each irradiance measurement. We selected the daily ozone value closest to the site of the spectrophotometer for each comparison. In practice, there could be a spatial offset between the ozone value and the irradiance measurement with which it is paired of as much as 1.8° in latitude and 1.6° in longitude, although these cases represent the extreme mismatches which occurred on only seven days. In addition, the temporal separation between the measured irradiance and the associated column ozone amount can be as large as five hours. Next, a wavelength-dependent attenuation by particulate matter, whose abundance varied over the period of observation, would appear as scatter in Figure 3.

[11] The effect of the errors identified above is surely smaller than that from short-term fluctuations in irradiance associated with rapidly changing cloudiness. There is a temporal separation of roughly 10 min between irradiance measurements at 305 and 345 nm. If horizontally inhomogeneous clouds in motion were present, the result would be an irradiance ratio in which numerator and denominator respond to slightly different configurations of clouds.

[12] A final option for explaining some of the scatter in Figure 3 involves the attenuation provided by clouds. The measurements in Figure 3 cover the full range of cloud cover encountered during the observing period, and it is possible that the irradiance ratio is affected by the presence of clouds. If the attenuation of irradiance associated with a cloudy sky is, in fact, wavelength-dependent, then this behavior will be implicit in Figure 3. By use of a suitably constructed regression model, it is possible to identify a link between $E_M(305, \theta)/E_M(345, \theta)$ and an index of cloudiness, irrespective of the other sources of scatter noted above.

[13] To characterize the degree of cloudiness, we define the "transmission ratio" at 345 nm as:

$$T(345) = E_M(345, \theta)/E_C(345, \theta) \tag{1}$$

where $E_C(345, \theta)$ is the irradiance that would have existed under a clear sky at the time and SZA of the 345 nm irradiance measurement. Obviously, $T(345) = 1.0$ corresponds to a clear sky, while a sky covered by thick clouds could have a value of 0.1 or less. To evaluate equation (1) we estimate $E_C(345, \theta)$ by performing a smooth fit of the form $E_C(345, \theta) = E_0 \exp[-\tau/(\cos\theta)]$ to a set of points chosen from Figure 1 and determining the coefficients E_0 and τ. The points selected were the ten largest irradiances measured in bins of width 0.05 in $\cos\theta$. The important outcome is to obtain values of $T(345)$ that respond only to changes in cloudiness and not to changes in SZA. A regression of the final $T(345)$ values against $\cos\theta$ verified that this was indeed the case.

[14] A regression model designed to detect wavelength dependence in the attenuation provided by cloudy skies must also account for absorption by ozone. An expression that accomplishes this is:

$$E_M(\lambda, \theta)/E_M(345, \theta) = T(345)^{\varepsilon(\lambda)} \exp[\alpha(\lambda) - \beta(\lambda)\Omega/(\cos\theta)] \tag{2}$$

or:

$$\ln[E_M(\lambda, \theta)/E_M(345, \theta)] = \alpha(\lambda) - \beta(\lambda)\Omega/(\cos\theta) + \varepsilon(\lambda)\ln[T(345)] \tag{3}$$

where Ω is total column ozone in DU and $\alpha(\lambda)$, $\beta(\lambda)$ and $\varepsilon(\lambda)$ are coefficients to be determined. The mathematical form of equation (3) relates irradiance to column ozone, SZA and cloudiness, while still being expressible as a linear regression model. The dependence on column ozone and SZA is compatible with theory, as illustrated in Figure 4. If $\varepsilon(\lambda) = 0$, the model forces the fractional attenuation due to sources other than slant path column ozone to be independent of wavelength. A value of $\varepsilon(\lambda)$ different from zero signifies wavelength-dependent attenuation, where $\varepsilon(\lambda) > 0$ implies a greater attenuation at λ than at 345 nm. We selected the form $T(345)^{\varepsilon(\lambda)}$ because it provides for a wavelength-dependent attenuation in the context of a linear regression model.

Table 1. Regression Coefficients and Standard Deviations Based on the Model: $\ln[E_M(\lambda, \theta)/E_M(345, \theta)] = \alpha(\lambda) - \beta(\lambda)\,\Omega/(\cos\theta) + \varepsilon(\lambda)\ln[T(345)]$

	Estimated Value of Parameter (Standard Deviation)		
Parameter	λ = 305 nm Band	λ = 310 nm Band	λ = 315 nm Band
$\alpha(\lambda)$	-1.70×10^{0} (3.24×10^{-2})	-1.39×10^{0} (2.50×10^{-2})	-1.22×10^{0} (2.08×10^{-2})
$\beta(\lambda)$	3.81×10^{-3} (7.90×10^{-5})	1.91×10^{-3} (6.10×10^{-5})	9.48×10^{-4} (5.08×10^{-5})
$\varepsilon(\lambda)$	1.23×10^{-1} (8.25×10^{-3})	3.87×10^{-2} (6.37×10^{-3})	-4.55×10^{-3} (5.31×10^{-3})[a]
$100r^2$ [b]	74.6%	53.5%	26.9%
$100r^2$ [c]	68.7%	51.7%	26.8%

[a]Not significant at the 95% level of confidence.
[b]Based on equation (3) in the text.
[c]Based on equation (3) in the text plus the constraint that $\varepsilon(\lambda) = 0$.

[15] Fits of equation (3) to the irradiance database for 305, 310 and 315 nm produced the values of $\alpha(\lambda)$, $\beta(\lambda)$, $\varepsilon(\lambda)$ and their standard deviations listed in Table 1. Table 1 also presents the percent of variance, $100r^2$, explained by equation (3) and by a simpler model which neglects wavelength dependence in the effect of clouds by setting $\varepsilon(\lambda) = 0$. The important results from Table 1 are as follows. First, all of the regression coefficients, with the exception of $\varepsilon(315)$, are significantly different from zero at a confidence level higher than 99%. Second, the dependence of the irradiance ratio on slant path column ozone, expressed by $\beta(\lambda)$, is consistent both in magnitude and wavelength dependence with expectations based on theory. This was confirmed by radiative transfer calculations analogous to those shown in Figure 4 for all wavelengths studied. Finally, the derived values $\varepsilon > 0$ indicate that, in the database as a whole, clouds provide a greater attenuation at 310 nm and 305 nm than at 345 nm. Furthermore, inclusion of the term that allows for a spectral dependence explains an increasing fraction of the variance as wavelength shrinks. The large standard deviation for $\varepsilon(315)$ precludes a judgment in this single case.

[16] The above analysis, which is based purely on statistical analysis of measurements, indicates that the attenuation of sunlight provided by cloudy skies varies with wavelength. However, the methodology provides no insight into the physical mechanisms involved. For this, a more detailed analysis that combines measurements and model-based calculations is called for.

4. Deductions Based on Combined Measurements and Theory

[17] Solar ultraviolet irradiance received by a horizontal surface is a sensitive function of SZA, while radiation at wavelengths shorter than 320 nm varies inversely with the column ozone amount, approximately 90% of which resides in the stratosphere. Since this research focuses on processes in the troposphere, it is desirable to develop a measure of ultraviolet irradiance that, for practical purposes, is independent of SZA and stratospheric ozone. The transmission ratio, defined in the previous section for 345 nm, can be generalized to all wavelengths studied:

$$T(\lambda) = E_M(\lambda, \theta)/E_C(\lambda, \theta, \Omega) \tag{4}$$

where $E_C(\lambda, \theta, \Omega)$ is the irradiance that would have existed under clear skies at the time of the measurement, and Ω is the column ozone amount. We use the radiative transfer model summarized by *Frederick and Erlick* [1995] with column ozone measurements from TOMS to compute a value of $E_C(\lambda, \theta, \Omega)$ that pairs with each measured irradiance in the spectrophotometer's data set. Care is required to ensure that the measured $E_M(\lambda, \theta)$ and computed $E_C(\lambda, \theta, \Omega)$ are indeed comparable since an offset between the absolute calibration of the spectrophotometer and the extraterrestrial solar irradiance used in the radiative transfer code will cause a systematic bias in the transmission ratios.

[18] In principle, values of $T(\lambda)$ computed for wavelengths where ozone absorbs are still insensitive to the atmospheric ozone amount. This is the case because absorption by ozone influences both the numerator and denominator in equation (4) to the same degree, although complications associated with the presence of clouds exist, as described later in this paper. Still, any errors in the TOMS ozone amounts used to generate $E_C(\lambda, \theta, \Omega)$ will lead to SZA-dependent biases. The solar backscatter method utilized by TOMS does not have high sensitivity to ozone located in the lower troposphere. This is true because the averaging kernels at wavelengths absorbed by ozone exhibit maxima in the lower stratosphere and are very small at altitudes below 5 km, even for clear skies. In addition, when clouds are present, the cloud top effectively acts as a lower-atmospheric boundary when viewed from space. Column ozone values obtained from the TOMS data set include contributions from the lower troposphere, but these are determined primarily by the ozone climatology input to the inversion algorithm rather than by information recorded by the sensor.

[19] It is inevitable that biases will exist between the transmission ratios deduced from irradiance measurements and those computed from the radiative transfer model, and some assumptions are necessary to account for these. We developed the following method on the basis of the requirement that a clear sky correspond to $T(345) = T(315) = T(310) = T(305) = 1$. When $T(345)$ was computed using clear-sky irradiances from the radiative transfer model, the 194 largest values fell in the range 1.0 to 1.2. The average of these was 1.041, which is slightly larger than the clear sky requirement of 1.0. We assume that these points, which compose about 20% of the database at 345 nm, correspond approximately to clear skies and that their average should in fact be 1.0. To achieve this, we divided all 958 $T(345)$ values by 1.041. Some of the final values still exceed 1.0, but irradiances larger than the clear-sky values can occur under partly cloudy skies when the solar disk is not obscured [*Frederick and Liao*, 2005]. We then extracted the values of $T(315)$, $T(310)$ and $T(305)$ that correspond to

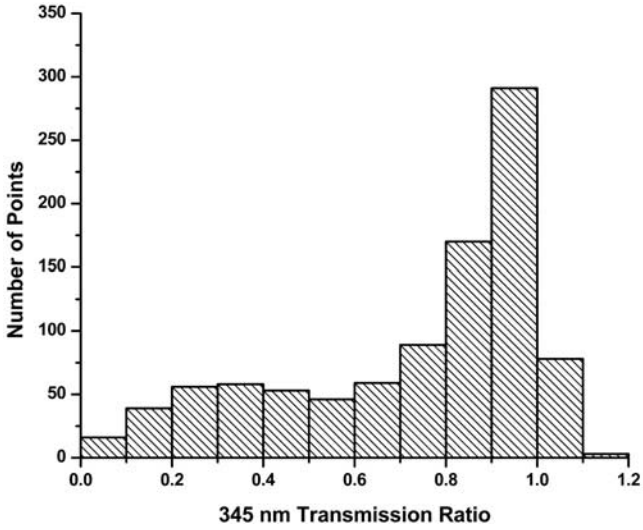

Figure 5. Histogram of transmission ratios for the 345 nm band. The plot includes a total of 958 measurements from May through September 2001.

the 194 largest values of $T(345)$. With the assumption that the average of these observations at each wavelength corresponds to clear skies, we required the mean of these 194 $T(315)$, $T(310)$ and $T(305)$ values to be 1.0, as was the case at 345 nm. This procedure resulted in dividing all transmission ratios computed from equation (4) by 1.007, 1.043 and 0.968 at 315, 310, and 305 nm, respectively. Although the above procedure, of necessity, contains subjective elements, no major conclusion of this work depends on details of the normalization.

[20] The transmission ratios, $T(345)$, $T(315)$, $T(310)$ and $T(305)$, with the normalization described above, form the basis of the analysis, where emphasis is placed on the longest and the shortest wavelength. Attenuation by clouds and aerosols alone determine the values of $T(345)$. The same processes influence $T(305)$, but absorption by lower-tropospheric ozone, that may differ from that implicit in the TOMS column value used to compute $E_C(\lambda, \theta, \Omega)$, is also a factor.

[21] Figures 5 and 6 are histograms of the transmission ratios based on all 958 irradiances measured in the 345 nm band and the 305 nm band, respectively. As noted previously, ratios in excess of 1.0 can occur on occasion. Values in the range 0.7–1.0 are the most frequent, while ratios less than 0.7 occur in roughly one third of the observations. The total number of points that fall between 0.7 and 1.0 is very similar at each wavelength, although the smaller end of this range appears more frequently for the shorter-wavelength band.

[22] Figure 7 depicts the relationship between transmission ratios for the 305 nm and 345 nm bands derived from each spectrophotometer scan, where logarithmic scales highlight behavior at small values, which correspond to dense clouds. The solid line in Figure 7 defines the case where no wavelength dependence exists, $\ln[T(305)] = \ln[T(345)]$. The open circles show the inequality $T(305) < T(345)$ to be typical and that $T(305)$ shrinks by a disproportionately large amount as $T(345)$ decreases. Figures 8 and 9, for the 310 nm and 315 nm wavelength bands, respectively, are analogous to Figure 7. These indicate a smooth wavelength dependence in the excess attenuation, with little or no difference between the results at 315 nm and 345 nm. The important information in Figures 7 and 8 arises from the nonlinear relationship between data at different wavelengths. This nonlinearity is unaffected by any normalization constants applied to the transmission ratios generated from equation (4).

[23] The apparent excess attenuation at 305 nm and 310 nm may arise from a problem in the analysis, or it

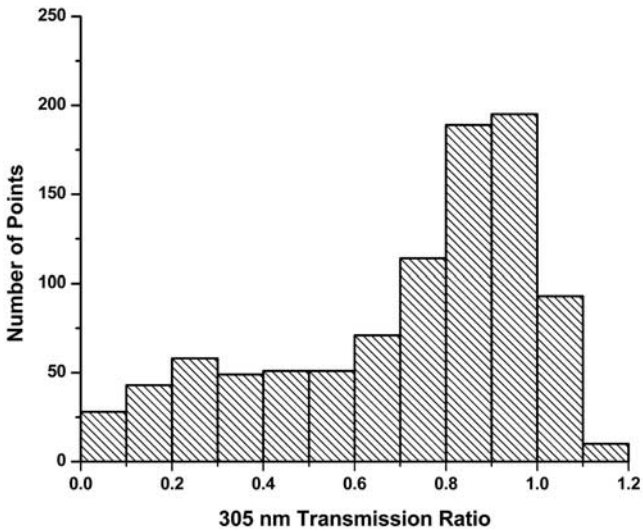

Figure 6. Histogram of transmission ratios for the 305 nm band. The plot includes a total of 958 measurements from May through September 2001.

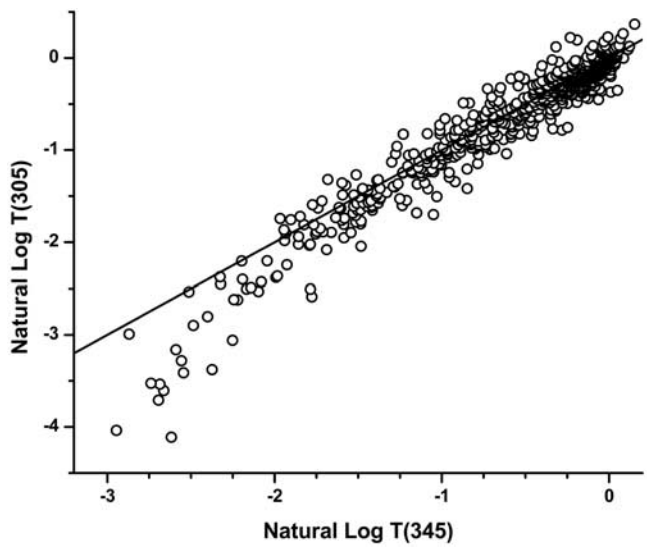

Figure 7. Transmission ratios in the 305 nm band plotted as a function of corresponding values for the 345 nm band for all points in the data set (open circles). The axes are expressed as natural logarithms to highlight the nonlinear behavior at small values, which correspond to thick cloud cover. The solid line defines the case $\ln[T(305)] = \ln[T(345)]$.

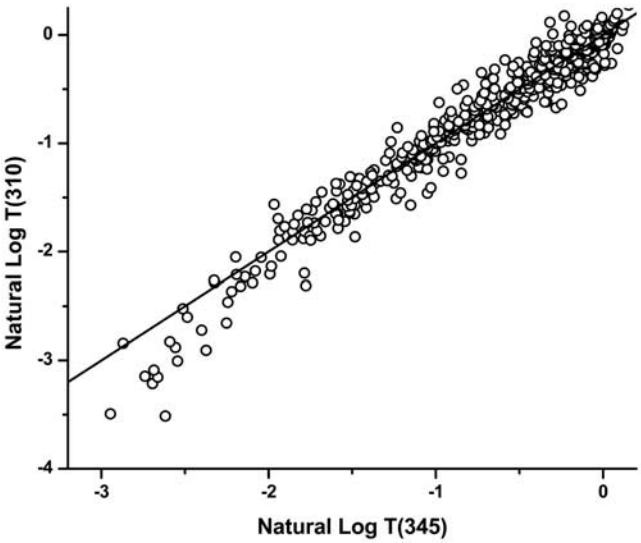

Figure 8. Transmission ratios in the 310 nm band plotted as a function of corresponding values for the 345 nm band for all points in the data set (open circles). The axes are expressed as natural logarithms to highlight the nonlinear behavior at small values, which correspond to thick cloud cover. The solid line defines the case ln[T(310)] = ln[T(345)].

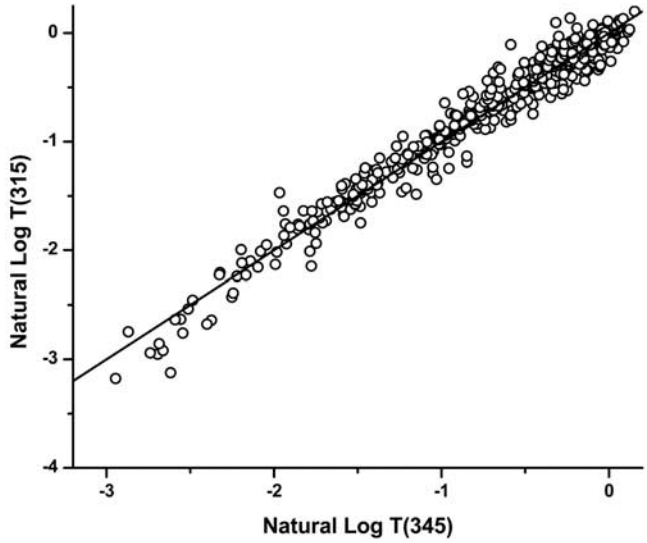

Figure 9. Transmission ratios in the 315 nm band plotted as a function of corresponding values for the 345 nm band for all points in the data set (open circles). The axes are expressed as natural logarithms to highlight the nonlinear behavior at small values, which correspond to thick cloud cover. The solid line defines the case ln[T(315)] = ln[T(345)].

may be a consequence of atmospheric processes. We here examine the first of these possibilities, emphasizing the 305 nm band. Satellite-based column ozone values enter Figure 7 through the computed clear-sky irradiance in the denominator of the transmission ratio, equation (4). The backscattered radiances measured by TOMS are sensitive to both the ozone amount and the lower boundary albedo in the instrument's field of view, particularly under conditions of thick cloud cover that produce small values of ln[T(345)]. If an error exits in the reported column ozone, and the magnitude of this error is correlated with the albedo, then the nonlinear behavior in Figure 7 might result. Specifically, if the column ozone value deduced from TOMS over dense cloud cover is smaller than the true value, then the computed transmission ratio at 305 nm will be too small as well, while that at 345 nm will be unaffected. We have no information to suggest that such an error indeed exists in the satellite-based results, but it is important to examine this option before seeking a physical explanation for the behavior in Figure 7.

[24] We performed a set of radiative transfer calculations to examine the hypothetical situation described above. These adopted typical midday summertime conditions for Chicago with the SZA being 32.3° and a column ozone value of 322.3 Dobson Units (DU). The cloudy-sky model of *Frederick and Erlick* [1995] treats a cloud as a diffusing surface, with an albedo A_c, placed at a specified altitude, and the transmission of the surface is $1 - A_c$. To simulate spectrophotometer measurements under extremely dense cloud cover, we adopted cloud albedos of A_c = 0.90 and 0.97 to compute ground-level irradiances for the 305 nm and 345 nm bands. The calculation of irradiances that would have existed under clear skies at the time of the spectrophotometer measurements arbitrarily assumes that column ozone deduced over dense clouds is only 294.0 DU. This column value corresponds to a vertical profile which contains only 10% of the true ozone amount at altitudes below 10 km and represents a scenario in which the satellite-based result erroneously contains very little tropospheric ozone when dense clouds are present. Such an error is unrealistically large, and we consider it here only in the context of an extreme case.

[25] Table 2 shows the simulated transmission ratios, as natural logarithms, computed from the radiative transfer model for the two cloud albedos considered here. Despite the extreme assumptions, the differences between simulated values of ln[T(345)] and ln[T(305)] are less than those displayed by the data. The column in Table 1 labeled "Observed ln[T(305)]" presents numbers derived from a quadratic fit to all of the points in Figure 7, $\ln[T(305)] = -0.0386 + 0.8729 \ln[T(345)] - 0.1258 \ln[T(345)]^2$. From this comparison, we conclude that reasonable errors in the column ozone values used to generate clear-sky irradiances are unable to account for the behavior in Figure 7.

[26] Absorption by ozone located in the lower troposphere, to which the TOMS measurements are insensitive, remains a potential explanation for the characteristics in Figure 7. This is a promising option because the computed clear-sky irradiances used in equation (4) do not include

Table 2. Sensitivity of the Transmission Ratio at 305 nm to an Error in Column Ozone Under Conditions of Thick Cloud Cover[a]

Cloud Albedo	Simulated[b] ln[T(345)]	Simulated[b] ln[T(305)]	Observed[c] ln[T(305)]
0.90	−1.98	−2.09	−2.26
0.97	−3.10	−3.25	−3.95

[a]The true ozone amount used to compute the numerator of T(305) is 322.3 DU. The value used to compute the denominator of T(305) is 294.0 DU, simulating a large error in column ozone deduced for cloudy conditions. See text for explanation.
[b]Based on equation (5) in the text.
[c]Based on a quadratic fit to the data in Figure 7 as given in the text.

enhanced ozone amounts typical of an urban boundary layer. As an initial test for a relationship, we fit a regression model of the form $\ln[T(305)] = a_0 + a_1\ln[T(345)] + a_2\chi$ to the database, where χ is the surface ozone mixing ratio measured on the rooftop adjacent to the spectrophotometer, and a_0, a_1 and a_2 are determined from the fit. The resulting value of a_2 was negative with very high statistical significance, although the percent of variance in $\ln[T(305)]$ explained by the surface ozone term was negligible.

[27] Motivated by this correlation, we performed a series of radiative transfer calculations that varied both cloudiness and the ozone mixing ratio in a 2 km thick layer adjacent to the ground. Recall here that the model treats a cloud as a diffusing surface where the sum of the albedo and transmission is unity. The objective was to determine if clouds located above a boundary layer containing enhanced ozone amounts could produce the behavior in Figure 7. The results showed that even a boundary layer mixing ratio of 90 ppbv, the largest recorded during the period of observation, could not lead to differences between $\ln[T(345)]$ and $\ln[T(305)]$ of the magnitude shown by the spectrophotometer data. Despite this negative result, the correlation between $\ln[T(305)]$ and surface ozone amounts suggests a link between tropospheric air quality and the characteristics of Figure 7. An acceptable physical mechanism must produce the inequality $\ln[T(305)] < \ln[T(345)]$ and nonlinear behavior in the range $-3 < \ln[T(345)] < -2$ which corresponds to thick cloud cover.

5. A Mechanism for Wavelength-Dependent Transmission Ratios

[28] The measurements reveal a wavelength-dependent absorption in association with very thick clouds, in excess of that which occurs under clear skies. Furthermore, the magnitude of this absorption decreases as wavelength increases from 305 nm to 315 nm, and the attenuation at 315 nm is only slightly greater than at 345 nm. The data do not allow conclusions on the existence or magnitude of absorption in the 345 nm band since this is the reference with which other spectral intervals are compared. The wavelength dependence of the absorption suggests a link to tropospheric ozone. Indeed, early calculations reported by *Frederick and Lubin* [1988] indicated that ozone in the interstitial air of a cloud leads to enhanced absorption as a consequence of the long effective geometrical path taken by sunlight through a medium that is optically thick in scattering. Independent results obtained since this work appear consistent with the mechanism [*Seckmeyer et al.*, 1996; *Mayer et al.*, 1998; *Erlick et al.*, 1998].

[29] To investigate the above possibility, we developed an analytic model of absorption by ozone within a plane parallel scattering slab, taken to represent a cloud. For simplicity the calculation assumes hemispherically isotropic radiances, including the light incident on the top of the slab. This model, while highly idealized, includes the essential physics of absorption within a cloud. A straightforward derivation based on the radiative transfer equation for a plane parallel, horizontally homogeneous medium yields the transmission of the cloud:

$$T_c(\lambda) = \left(\kappa^2 - 1\right)/\left[\kappa^2 \exp(\Gamma\tau^*) - \exp(-\Gamma\tau^*)\right] \quad (5)$$

where

$$\Gamma = \left(\eta^2 - \gamma^2\right)^{1/2} \quad (6)$$

$$\kappa = \left[(\eta+\gamma)^{1/2} + (\eta-\gamma)^{1/2}\right]/\left[(\eta+\gamma)^{1/2} - (\eta-\gamma)^{1/2}\right] \quad (7)$$

$$\eta = 2(1 - f\omega) \quad (8)$$

$$\gamma = 2\omega(1 - f) \quad (9)$$

The optical properties of the slab are characterized by the total optical depth τ^*, the single scattering albedo ω, and the forward scattering fraction f, being the probability that scattering leads to radiation propagating into the forward hemisphere as defined relative to the direction of energy flow prior to scattering. The cloud model adopts the value $f = 0.9$. The optical thickness of the cloud for scattering alone is $\tau_s = \tau^*/\omega$.

[30] The calculations assume the scattering optical depth associated with cloud droplets to be the same at 305 nm and 345 nm and that the mixing ratio of ozone, χ, is constant throughout the cloud. For a slab of geometrical thickness Δz, the single scattering albedo is:

$$\omega = \tau_s/\{\tau_s + \sigma(\lambda)\chi[M]\Delta z\} \quad (10)$$

where $\sigma(\lambda)$ is the absorption cross section of ozone at wavelength λ from the work of *Molina and Molina* [1986], and $[M]$ is the average atmospheric number density over the vertical extent of the cloud. The model assumes $[M]\Delta z$ to be proportional to τ_s and thereby yields a single scattering albedo that is constant in altitude through the cloud.

[31] The quantity $T_c(\lambda)$ in equation (5) measures the attenuation of surface irradiance associated with cloudy skies, and it is appropriate to compare predictions from it with the empirical values in Figure 7, subject to recognition that the model is highly simplified. A more detailed treatment would have to include the coupling between molecular scattering and reflection from the cloud base [*Frederick and Erlick*, 1997; *Kylling et al.*, 1997], but the fact that excess absorption arises from multiple scattering within the cloud would remain valid. Figure 10 presents computed values of $\ln[T_c(305)]$ plotted against the corresponding values of $\ln[T_c(345)]$ for two ozone mixing ratios in the cloud, χ = 30 ppbv and 90 ppbv. The results display a nonlinear relationship that agrees extremely well with that in Figure 7. When $\ln[T_c(345)] = -3$, the model yields $\ln[T_c(305)] = -3.48$ and -4.27 for the smaller and larger ozone mixing ratio, respectively. Furthermore, the computed values appear nearly linear over the range $-2 < \ln[T_c(345)] < 0$, with nonlinearity developing when $\ln[T_c(345)] < -2$. On the basis of these results and the wavelength dependence apparent in Figures 7–9, it appears reasonable to attribute the behavior deduced empirically to absorption by ozone contained within the clouds observed by the spectrophotometer. While the above explanation produces results consistent with the observations, it does not constitute a proof that ozone alone is the causal agent. We cannot

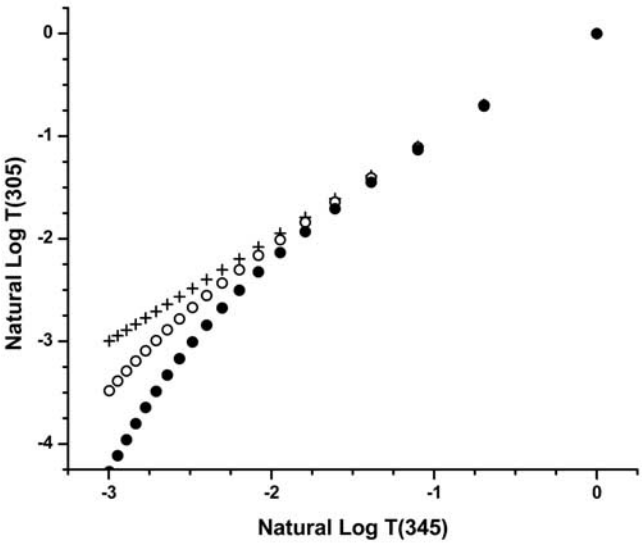

Figure 10. Transmission of a slab taken to represent scattering and absorption within a cloud. Computed transmissions for the 305 nm band are plotted as a function of those for the 345 nm band, expressed as natural logarithms. Open and solid circles assume the ozone mixing ratio in the modeled cloud to be 30 ppbv and 90 ppbv, respectively. Pluses define the case $\ln[T(305)] = \ln[T(345)]$.

disregard the possibility of wavelength-dependent attenuation associated with particulate matter [*Jacobson*, 2001] or species dissolved in cloud water.

6. Conclusions

[32] Measurements from the Chicago-based Brewer spectrophotometer combined with radiative transfer calculations produce transmission ratios in the 305 nm wavelength band that are generally smaller than those for the 345 nm band under the most dense clouds. Results for the 310 nm and 315 nm bands indicate a smooth wavelength dependence in this excess absorption. The nonlinear behavior in Figures 7 and 8 implies that the observed differences cannot result from fixed, but wavelength-dependent, offsets in the computed transmission ratios.

[33] A simple model of absorption and scattering within a cloud produces results that are consistent with the observations. These reveal a likely coupling between the ultraviolet transmission properties of clouds and the ozone content of the troposphere. The combination of a gaseous absorber and a medium that is optically thick in scattering leads to a greater attenuation than when the same quantity of absorber exists in clear air. The observed excess attenuation near 305 nm and 310 nm, if it is the result of absorption by ozone, indicates enhanced production of $O(^1D)$, and therefore altered photochemical activity, in clouds.

[34] **Acknowledgments.** Although the research described in this article has been funded wholly or in part by the United States Environmental Protection Agency through grant CR-83089001-0 to the University of Chicago, it has not been subjected to the Agency's required peer and policy review and therefore does not necessarily reflect the views of the Agency and no official endorsement should be inferred. One of the authors (S.W.) acknowledges support from the Department of Energy in the form of a Graduate Research Environmental Fellowship.

References

Barnard, W. F., V. K. Saxena, B. N. Wenny, and J. J. DeLuisi (2003), Daily surface UV exposure and its relationship to surface pollutant measurements, *J. Air Waste Manage. Assoc.*, *53*, 237–245.

Bordewijk, J. A., H. Slaper, H. A. J. M. Reinen, and E. Schlamann (1995), Total solar-radiation and the influence of clouds and aerosols on the biologically effective UV, *Geophys. Res. Lett.*, *22*, 2151–2154.

Bruel, C., and P. J. Crutzen (1989), On the disproportionate role of tropospheric ozone as a filter against solar UV-B radiation, *Geophys. Res. Lett.*, *16*, 703–706.

Erlick, C., and J. E. Frederick (1998), Effects of aerosols on the wavelength dependence of atmospheric transmission in the ultraviolet and visible: 2. Continental and urban aerosols in clear skies, *J. Geophys. Res.*, *103*, 23,275–23,285.

Erlick, C., J. E. Frederick, V. K. Saxena, and B. N. Wenny (1998), Atmospheric transmission in the ultraviolet and visible: Aerosols in cloudy atmospheres, *J. Geophys Res.*, *103*, 31,541–31,555.

Frederick, J. E., and C. Erlick (1995), Trends and interannual variations in erythemal sunlight, 1978–1993, *Photochem. Photobiol.*, *62*, 476–484.

Frederick, J. E., and C. Erlick (1997), The attenuation of sunlight by high-latitude clouds: Spectral dependence and its physical mechanisms, *J. Atmos. Sci.*, *54*, 2813–2819.

Frederick, J. E., and Y. Liao (2005), Photosynthetically active sunlight at high southern latitudes, *Photochem. Photobiol.*, *81*, 603–608.

Frederick, J. E., and D. Lubin (1988), The budget of biologically active ultraviolet radiation in the Earth-atmosphere system, *J. Geophys. Res.*, *93*, 3825–3832.

Frederick, J. E., A. E. Koob, A. D. Alberts, and E. C. Weatherhead (1993), Empirical studies of tropospheric transmission in the ultraviolet: Broadband measurements, *J. Appl. Meteorol.*, *32*, 1883–1892.

Jacobson, M. Z. (2001), Global direct radiative forcing due to multicomponent anthropogenic and natural aerosols, *J. Geophys. Res.*, *106*, 1551–1568.

Kerr, J. B., and C. T. McElroy (1995), Total ozone measurements made with the Brewer ozone spectrophotometer during STOIC 1989, *J. Geophys. Res.*, *100*, 9225–9330.

Kerr, J. B., C. T. McElroy, D. I. Wardle, R. A. Olafson, and W. F. J. Evans (1985), The automated Brewer spectrophotometer, in *Atmospheric Ozone*, edited by C. S. Zerefos and A. Ghazi, pp. 396–401, Springer, New York.

Kylling, A., A. Albold, and G. Seckmeyer (1997), Transmittance of a cloud is wavelength-dependent in the UV-range: Physical interpretation, *Geophys. Res. Lett.*, *24*, 397–400.

Mayer, B., A. Kylling, S. Madronich, and G. Seckmeyer (1998), Enhanced absorption of UV radiation due to multiple scattering in clouds: Experimental evidence and theoretical explanation, *J. Geophys. Res.*, *103*, 31,241–31,254.

Molina, L. T., and M. J. Molina (1986), Absolute absorption cross sections of ozone in the 185- to 350- nm wavelength range, *J. Geophys. Res.*, *91*, 14,501–14,508.

Repapis, C. C., H. T. Mantis, A. G. Paliatsos, C. M. Philandras, A. F. Bais, and C. Meleti (1998), Case study of UV-B modification during episodes of urban air pollution, *Atmos. Environ.*, *32*, 2203–2208.

Schafer, J. S., V. K. Saxena, B. N. Wenny, W. Barnard, and J. J. DeLuisi (1996), Observed influence of clouds on ultraviolet-B radiation, *Geophy. Res. Lett.*, *23*, 2625–2628.

Seckmeyer, G., R. Erb, and A. Albold (1996), Transmittance of a cloud is wavelength-dependent in the UV-range, *Geophys. Res. Lett.*, *23*, 2753–2755.

J. E. Frederick and S. Winiecki, Department of the Geophysical Sciences, University of Chicago, 5734 South Ellis Avenue, Chicago, IL 60637-1434, USA. (frederic@uchicago.edu; shelby@alumni.uchicago.edu)